Advanced Steel Construction – Vol. 21 No. 1 (2025) 64–72
DOI:10.18057/IJASC.2025.21.1.6

METHOD OF IMPERFECTION RANDOM FIELD CONSTRUCTION FOR WELDED CYLINDRICAL SHELL BASED ON SMALL SAMPLE

Hong-Fei Fu [1], Yu-Hong Shi [1,*], Wei-Xiu Xv [1], Fan Yang [1], Hao Yang [2] and Liang-Liang Jiang [1]

[1] *Beijing Institute of Astronautical Systems Engineering, Beijing 100076, China*
[2] *State Key Laboratory of Structural Analysis, Optimization and CAE Software for Industrial Equipment, Dalian University of Technology, Dalian 116023, China*
** (Corresponding author: E-mail: 19217049700@163.com)*

ABSTRACT

The initial geometrical imperfections of thin-walled cylindrical shell structures are important factors that cause the actual bearing capacity of such products to deviate from the theoretical value. In recent years, with the development of digital image measurement technology, it is possible to obtain geometric imperfections(GIs) through the measurement of the real geometric shape of the product, and it is possible to accurately predict the structural load-bearing capacity by considering the imperfections. On this basis, the initial GIs random field can then be considered to carry out thin-walled cylindrical shell load carrying capacity simulation targeting to obtain the strength distribution, and the lower limit of structural strength can be determined scientifically through a probabilistic approach..In this paper, based on Fourier series method, a modeling method of imperfection random field considering geometrical imperfection features is proposed for welded plates of carrier rocket tank. In the first stage, in order to solve the problem of large GIs characterization parameters, a GIs characterization method based on simplified Fourier coefficients is proposed, and an evaluation criterion based on determination coefficient (R^2) and characterization accuracy (RP) is established. In the second stage, according to the simplified GIs, a dual construction method based on the waveform and amplitude of the distribution of sample GIs is innovatively proposed. And according to the structural characteristics, a single panel is used as a sample to achieve sample expansion. It solves the problem of uncertain random field construction of such structure morphology under the condition of small sample. Finally, the method is applied to the actual engineering structure, and the accuracy of the method is verified by the bearing capacity test data.

ARTICLE HISTORY

Received: 14 July 2024
Revised: 15 December 2024
Accepted: 16 December 2024

KEYWORDS

Plate welding;
Thin-walled cylindrical shell;
Geometric imperfections;
Random field;
Small sample

1. Introduction

Thin-walled structures are widely used in space vehicles due to light weight and high load-bearing efficiency [1,2]. There are many failure modes for thin-walled structure while compressive buckling is the main one. Basically, the theoretical buckling load depends on the structural dimensions and mechanical properties of material [3,4]. There exists certain random geometrical imperfections in dimension, surface quality etc., which could cause bearing capability deviation in thin-walled structures with the same design scheme. This uncertainty from geometric imperfections attracted NASA's attention since 1960s. The engineers in NASA introduced the reduction coefficient into buckling bearing evaluation for thin-walled structures, and provided the envelope on the buckling bearing capacity with sufficient engineering data subsequently [5]. With the development of product processing and quality control technology, structural products based on this envelope design have become so conservative to the improvement of structural bearing efficiency [6,7].

In order to predict more reasonable load response of thin-walled structures, many researchers have studied the effect of GIs on the bearing capacity. Based on the random field signatures of the GIs distribution of thin-walled structures, it mainly focuses on the imperfections distribution form and amplitude.In the early stage, due to the limitation of measurement means, the imperfection form was mainly based on the assumption when the real geometry of the structure was unknown. The influence trend of different imperfection amplitudes on carrying capacity was analyzed. Huhne [8] proposed a Single Perturbation Load Approach(SPLA), which uses radial concentrated force in the structure to cause a single dimple imperfection. On this basis, Wang et al.[9] developed it into the the worst multiple perturbation load approach to obtain the lower limit of structural bearing capacity.In order to study the influence of the most unfavorable imperfections, Schmidt et al.[10] introduced the structural buckling waveform, the most serious imperfection form, into the finite element model as the initial GIs.Based on this, the influence trend of different amplitude values on the bearing capacity was analyzed, and the lower limit of the structural bearing capacity was obtained.With the development of digital measurement technology, the real geometric shape deviation of products can be obtained by scanning measurement, and it can be introduced into the ideal finite element model to achieve fine analysis of carrying capacity.Many scholars such as Arbocz and Elishakoff [11-13] obtained the product GIs based on the measured geometric morphology data, and studied the GIs characterization method by Fourier series fitting. The GIs were introduced into the ideal finite element model to achieve the accurate calculation of the structure bearing capacity considering the measured morphology.

Based on the measured geometric deviation samples of the product, the study of the distribution characteristics of the total geometric deviation random field is the key to realize the uncertainty analysis of the thin-walled structure bearing [14,15]. Describing the distribution information of product imperfection field requires a large amount of data, and how to reasonably reduce the variable dimension and efficiently construct the imperfection random field model has become the key to study the uncertainty of morphology [16,17].With the well-known Karhunen-Loeve (KL) transform [18], the processing method of generating random variables through orthogonal transformation and greatly reducing the dimension of data set has been widely used in random field models.On this basis, Ghanem and Spanos [19] proposed a piecewise basis function to describe random fields. Li and Kiureghian et al. [20] proposed the Optimal linear estimation method (OLE) and the improved expension OLE method (EOLE). Random fields are described in terms of random variables and shape functions.This idea gradually developed into the mainstream method of structural imperfection random fields [21-23].

The geometrical imperfection random field of thin-walled structures is often assumed to be a two-dimensional Gaussian random process, and the relevant parameters need to be determined during characterization. Yang Hao [24] et al. proposed a two-stage random field parameter estimation method by quantifying the imperfection uncertainty, so as to achieve accurate prediction of random field characterization parameters. M. Fina and P. Weber et al. [25] extended the probabilistic method into a fuzzy process, fully considering the uncertainty of samples. However, this method introduces more variables and emphasizes the sensitivity analysis between variables, which undoubtedly increases the calculation cost. Limited by high cost, the samples and test data of thin-walled structures under the same conditions are limited. Under the condition of finite samples, Schenk and Christian et al. [26] used the KL expansion theory and Gaussian random process to give the second-order moment characteristics of the limit load through direct Monte Carlo simulation. Li et al. [27] proposed using maximum entropy distribution to estimate the probability density function of random variables, avoiding the introduction of Gaussian distribution hypothesis, and extending the equality constraint to an interval form to adapt to small sample conditions.

Some existing random field models do not give too much consideration to the sample structure and processing mode. In order to obtain as many test samples as possible, products with similar conditions are used as training samples to establish a unified random field model.However, in engineering, the imperfection features of products under some processing and forming processes have typical specificity. For example, the tank body of a large-diameter launch vehicle is generally welded by several wall plates after processing. The welding residual stress and the changes of bending stiffness at the welding position lead

to obvious mutation of GIs field at the welding position, which affects the overall imperfection features [11]. At the same time, due to high manufacturing and testing costs, the number of samples of the same product is limited. In this paper, a Fourier series geometric imperfection random field construction method is innovatively proposed for welded structures of panels, using a structural single-wall panel as a research sub-sample. The structure GIs distribution features and deviation amplitude law are studied, and the random field model suitable for the geometric uncertainty of small sample products is constructed, which has more practical engineering application value.

The content of each part of the article is summarized as follows. In section 2, the principle of Fourier series characterizing imperfections and its simplification method are introduced; Section 3 establishes the novel dual modelling method of imperfection random field proposed in this paper; Section 4 establishes a Fourier random field model with measured geometric imperfections of cylindrical shells, and verifies the validity of the model by combining with the results of the structural physical tests, and the characteristics of the sample imperfections, the effect of each feature on the load bearing are analysed; Finally, conclusions are drawn and the value of the study is illustrated in Section 5.

2. Fourier series-based geometric imperfections characterization method of thin-walled cylindrical shells

2.1. Extraction of geometric imperfections of thin-walled cylindrical shells

The radial deviation referenced to the ideal surface of the thin-walled structure can induce buckling failure[28]. Therefore, it is necessary to define and reconstruct the surface of imperfection. In this work, the morphological data of the thin-walled cylindrical structure was obtained by employing three-dimensional laser scanning technology. The radial deviation of point cloud data is expressed as the off-surface deviation value.

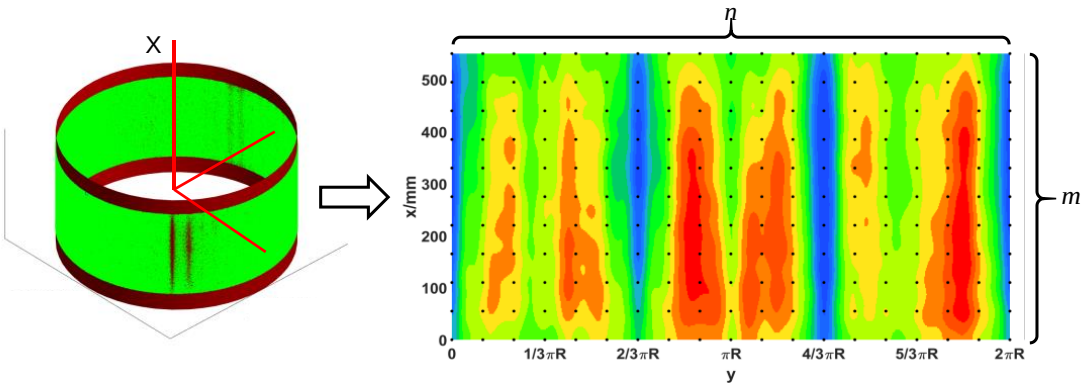

Fig. 1 Off-surface deviation contour of the outer surface

For the convenience to analyze the imperfection information, the radial deviation data was plotted as contour in Fig. 1. Based on the observation position of each measuring point, the structural imperfection was described by *m* off-surface deviation values in the axial direction and *n* off-surface deviation values in circumferential direction, respectively. The original off-surface deviation field was eventually expressed as two-dimensional matrix **w(x,y)** (as Eq. (1)).

$$\mathbf{w(x,y)}=\begin{bmatrix} w(x_1,y_1) & w(x_1,y_2) & \cdots & w(x_1,y_n) \\ w(x_2,y_1) & w(x_2,y_2) & \cdots & w(x_2,y_n) \\ \vdots & \vdots & \ddots & \vdots \\ w(x_m,y_1) & w(x_m,y_2) & \cdots & w(x_m,y_n) \end{bmatrix} \tag{1}$$

2.2. Fourier series-based representation method on imperfection field

Fourier series method is widely used to describe the initial GIs of cylindrical shells [29]. To efficiently represent imperfection field, the Fourier series method was employed in this work. Circumferential imperfection can be represented by the superposition of trigonometric functions with different periods and amplitudes at a fixed axial coordinate. The axial principle is similar, traversing through the coordinates of each point cloud to complete the representation of the imperfection field. Therefore, double Fourier series was employed to fit the off-surface deviation values of each scatter point as:

$$\begin{aligned} w(x_p,y_q) &= t\cdot\sum_{k=0}^{n_1}\sum_{l=0}^{n_2}\cos\frac{k\pi x_p}{L}\left(A_{kl}\cos\frac{ly_q}{R}+B_{kl}\sin\frac{ly_q}{R}\right) \\ &= t\cdot\sum_{k=0}^{n_1}\sum_{l=0}^{n_2}\gamma_{kl}\cos\frac{k\pi x_p}{L}\sin\left(\frac{ly_q}{R}+\theta_{kl}\right) \end{aligned} \tag{2}$$

Where A_{kl} and B_{kl} are the coefficients of Fourier series; *k* and *l* are the axial half-wave number and circumferential full wave number under the Fourier order respectively; By means of series fitting, the GIs information of the structure is retained in each order coefficient. For ease of analysis, the double series is expressed as wave peak value $\gamma_{kl}=\sqrt{A_{kl}^2+B_{kl}^2}$ and phase angle θ_{kl}. Fourier series method superimposes multi-order axial and circumferential waves. Respectively represent the imperfection information in the corresponding direction. The detailed principle is shown in Fig. 2.

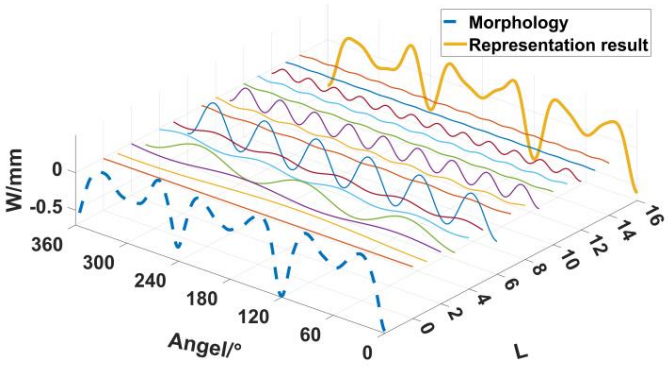

Fig. 2 Schematic diagram of imperfection expressed by Fourier series

The trigonometric function values **s(k, l)** for different *k* and *l* values were calculated and combined with the off-surface deviation matrix **w(x, y)**. Through singular value decomposition of the augmented matrix [**w(x, y) s(k, l)**], simple wave of Fourier periodic signals are obtained, and the Fourier series characterization of GI field is realized by extracting the coefficients of each term.

Affected by the production and processing methods, the surface imperfection signature of similar structural products have certain regularity. Fourier series method decouples the product axial and circumferential signature. The complex structural imperfections field is described by a relatively clear superposition of simple wave of each period.

2.3. Simplification on Fourier series of GIs field

According to the method mentioned above, there will be more than thousand coefficients used in the Fourier series. The Fourier coefficients A_{kl} and B_{kl} in Eq. (2) are a set of constants, reflecting the contribution from different periodic trigonometric functions to the overall GIs. In this work, the dominant coefficients which contribute the main trend of the GIs will be kept in order to reduce the complexity of calculation. If the integral values of the sine and cosine functions are equal in the whole period, the corresponding coefficients from the sine and cosine parts contribute equally to the imperfection field. Therefore, there are three methods to simplify the Fourier series as following:

1. Use the peak value of the wave γ_{kl} as the simplification factor;
2. Use the A_{kl} and B_{kl} as the simplification factor;
3. Use the group of coefficients [A_{kl} B_{kl}] as the simplification factor.

Since there are limited structures to collect the imperfection data, it should be reasonable to choose the simplification method according to the actual situation. First of all, the deviation measures were calculated for each simplification method. Then, the coefficients A_{kl} and B_{kl} of larger absolute deviation values were saved to represent the contribution from the corresponding series. Finally, the imperfection result from the simplified Fourier series was compared with the original one to ensure the accuracy of simplification.

Define μ_w as the mean of the off-surface deviation matrix, which is expressed as Eq. (3). A determination factor R^2 is defined subsequently as Eq. (4), which is used as the evaluation criterion of the fitting accuracy about Fourier series.

$$\mu_w = \frac{1}{m \times n} \sum_{p=1}^{m} \sum_{q=1}^{n} w(x_p, y_q) \tag{3}$$

$$R^2 = 1 - \frac{\sum_{p=1}^{m} \sum_{q=1}^{n} \left(\tilde{w}(x_p, y_q) - w(x_p, y_q)\right)^2}{\sum_{p=1}^{m} \sum_{q=1}^{n} \left(\tilde{w}(x_p, y_q) - \mu_w\right)^2} \tag{4}$$

Where $\tilde{w}$ is the deviation value from the simplified Fourier series; w is the true value from the structure.

The overall fitting accuracy is defined as the minimum value in limited samples, which indicates $R^2 = \min R_i^2$ .The calculation efficiency of three methods is compared to determine the optimal method at the same accuracy although the numbers of dominant coefficients are different. Eventually, the off-surface deviation after simplification is expressed as:

$$w(x_p, y_q) \approx t \cdot \sum_{k=0}^{n_1'} \sum_{l=0}^{n_2'} \cos\frac{k\pi x_p}{L} \left(A'_{kl} \cos\frac{ly_q}{R} + B'_{kl} \sin\frac{ly_q}{R} \right) \tag{5}$$

Where n_1' and n_2' are the numbers of retained parts after simplification; A'_{kl} and B'_{kl} represent the coefficients after simplification.

An criterion on structural bearing capacity is defined in order to ensure the accuracy of simplification which is:

$$RP = \frac{|P_{cr} - P_{cs}|}{P_{cr}} \le \zeta \tag{6}$$

Where P_{cr} is the critical load before simplification, and P_{cs} is the critical load after simplification. ζ is critical value to evaluate the accuracy on the simplification, which was 1% in this work.

The during the procedure in the following context, the value of R^2 will be increased until the *RP* criterion is met.

3. Construction method of Fourier series-based imperfection random field

Since there are extremely limited structures as samples in actual engineering (only three in this work). Some literature [30-32] shows that the structure welded by plates shows a trend of convex outside the welding area and concave inside the weld, and the imperfection signature have obvious rules. Taking Fourier coefficient as the control variable of imperfection random field, Fourier coefficient can reflect the imperfection signature of a class of structures [33]. Therefore, an imperfection random field model was proposed to describe the uncertainty from the imperfections in this work. The flowchart is shown as Fig. 3.

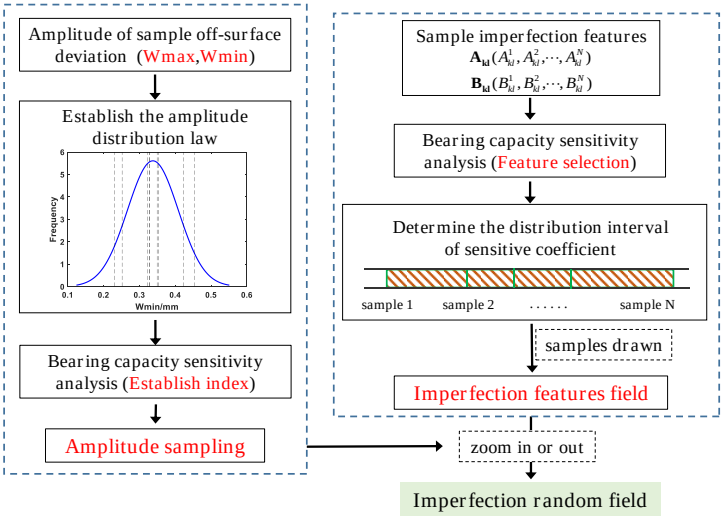

Fig. 3 Imperfection random field modeling method

First of all, the statistic distribution about Fourier series coefficients of same order in all samples are calculated according to the features of the imperfection wave. The random uniform sampling is carried out within the coefficient distribution interval to determine the imperfection features of the random field.

Then, the amplitude distribution of the imperfections random field is established based on the imperfections amplitude rule of the existing samples. Amplitude sampling was carried out within a certain confidence interval. Avoid situations where random field results deviate from the sample range due to adequate sampling.

According to the analysis about Fourier series, the trigonometric functions of each order represent independent imperfection features. The corresponding coefficients represent the proportion of imperfection features. The GIs of the sample is represented in the form of simplified series with different weights according to the specific weight ratio. Before sampling, the variable range was determined with the minimum value and maximum value in three samples for each coefficient. Then, uniform sampling was performed randomly in the range for all coefficients to construct the Fourier series-based imperfection,as Eq. (7).

$$\hat{A}_{kl} \in \left[\min A_{kl}^i, \max A_{kl}^i\right]$$

$$\hat{B}_{kl} \in \left[\min B_{kl}^i, \max B_{kl}^i\right]$$

$$\hat{w}(x_p, y_q) = t \cdot \sum_{k=0}^{n_1'} \sum_{l=0}^{n_2'} \cos\frac{k\pi x_p}{L} \left(\hat{A}_{kl} \cos\frac{ly_q}{R} + \hat{B}_{kl} \sin\frac{ly_q}{R} \right) \tag{7}$$

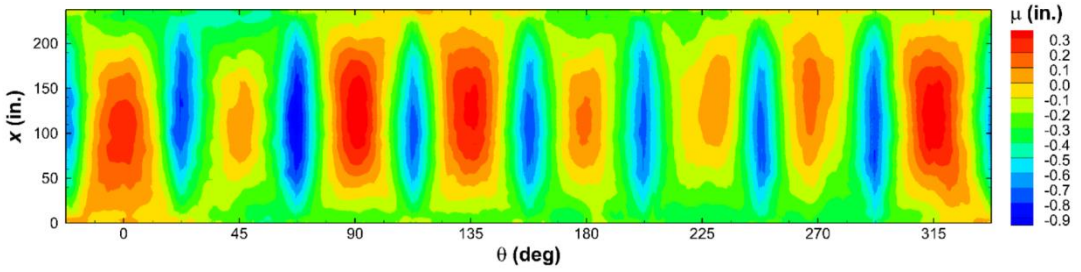

Fig. 4 Off-surface deviation field of welded plate structure [30]

In order to ensure that the amplitude of the imperfection field does not deviate from the statistical result of the sample, the amplitude of the off-surface deviation of the sample is measured under certain confidence requirements.According to the statistical results, the sampled off-surface deviation field is enlarged or reduced to realize the amplitude rule control of the imperfection random field.

For instance, Fig.4. shows the surface imperfections of the welded structure of eight plates measured by NASA [34]. It is obvious that it shows concave at weld line and convex in the middle of the shell between neighbored weld lines. In order to reflect the detail features about sample amplitude, the amplitude of the off-surface deviation in a single plate was taken as an independent statistical sample. The distributions about the minimum off-surface deviation values

$\min \hat{w}(x_p, y_q)$ and maximum off-surface deviation values $\max \hat{w}(x_p, y_q)$ of the single plate were tested respectively. The probability distribution model of the amplitude was established. According to its distribution features, random field amplitude sampling is carried out within the confidence interval [μ-3σ, μ+3σ] of the amplitude statistics results with 99.7 per cent confidence level, and the preliminary constructed defective feature field was deflated. The imperfection feature field constructed initially is scaled.

Taking the minimum off-surface deviation as an example, the scaled imperfection random field is expressed as:

$$\mathbf{w}_L(\mathbf{x},\mathbf{y}) = \frac{\tau}{\min \hat{w}(x_p, y_q)} \hat{\mathbf{w}}(\mathbf{x},\mathbf{y}) \tag{8}$$

Where, τ is the concave amplitude of the sample within the statistical range of the sample.The sensitivity analysis about the scaled maximum and minimum deviations were performed respectively. In order to ensure computational efficiency, global sampling was employed according to the features of the probability distribution model of $\min \hat{w}(x_p, y_q)$ and $\max \hat{w}(x_p, y_q)$. The corresponding sample of amplitude $\boldsymbol{\tau} = (\tau_1, \tau_2, \cdots, \tau_L)$ was obtained. Each bearing capacity $P(\tau_j)$ of the structure was calculated accordingly. The essential effect size of sample *i* is defined as:

$$EE_i = \frac{1}{q} \sum_{j}^{q} \left| \frac{P(\tau_j) - P_{cl}}{(\tau_j - \min \hat{w}(x_p, y_q)) / \min \hat{w}(x_p, y_q)} \right| \tag{9}$$

According to the mean value of the essential effect values of each sample, the sensitivities of two types of amplitudes on the bearing capacity were compared. The index with higher sensitivity was selected as the scaled standard. After amplitude sampling is introduced, the sampling results of the imperfection random field model include the basic features of the sample imperfections, and ensure that the imperfection amplitude falls within the confidence range of the sample. By Eq. (2), the values of random field off-surface deviation are expressed in Fourier series.The scatter field is fitted to the form of space surface to represent the imperfection, and the imperfection feature field is constructed based on Fourier series method.The operation process of this method is relatively simple,has clear the physical features, and it is suitable for all kinds of sample conditions.Especially for products with the same structural form and process, the random field model can fully include the imperfection features of such products.

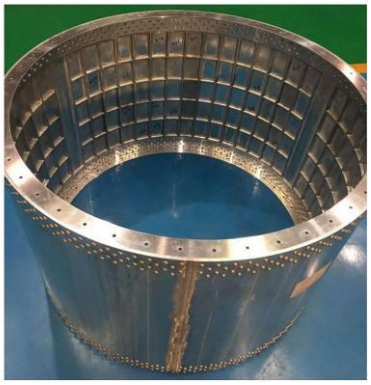

Fig. 5 Plate welded thin-walled cylinders

4. Results and discussions

As shown in Fig. 5, there are there structures used to verify the method in the following context. All of them are orthogrid-stiffened aluminum cylinders of 1m in diameter. The structure is divided into three aluminum shell parts which are welded together, and steel end rings which connect to the outer surface both ends of the cylinder. The overall height of the cylinder and the orthogrid-stiffened part are 710mm and 550mm, respectively. The thickness of the stringer is 2mm. A total of 3 products were produced, and the material properties, structural dimensions and GIs of each product were measured.

4.1. Measured product geometric imperfections and their bearing capacity

Abaqus was used to model and analyze the bearing capacity of the structure. As comparison, the bearing capacity of the ideal structure with smoothing surface was 3109.2 kN from simulation. Three weld lines failed first which caused the overall failure subsequently. The relative error of the bearing capacity was 9.10% between the ideal structure and the average of three samples from experiments.

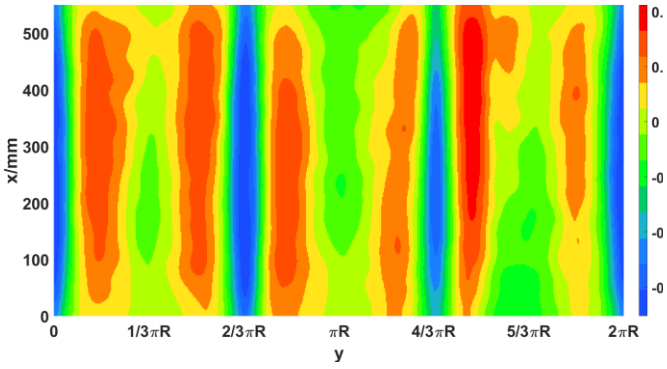

(a) Structure1

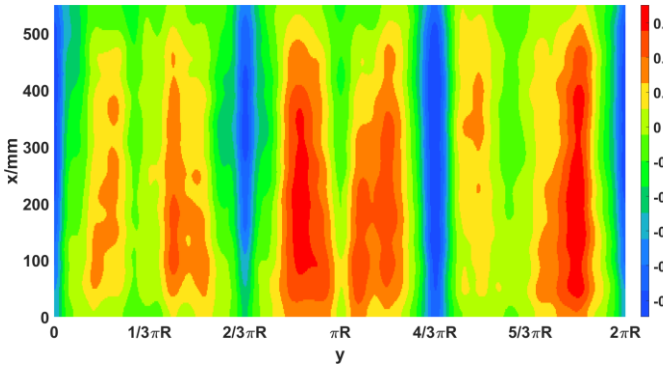

(b) Structure2

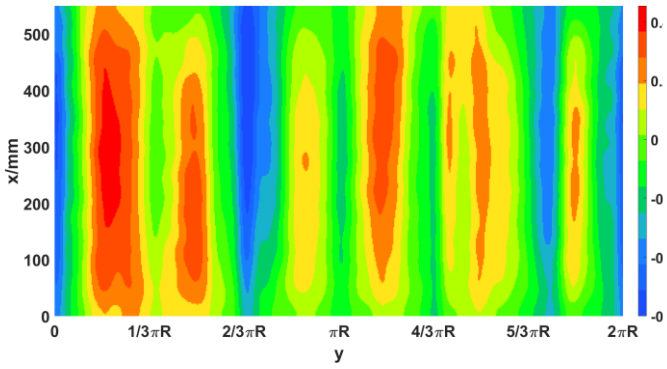

(c) Structure3

Fig. 6 Measured GIs of the product

Three-dimensional laser scanning technology was used to obtain the GIs information of each physical structure. The GIs were expressed as off-surface deviation normalized by thickness $^*t = 2$ of the structure , as shown in Fig.6. When the fitting accuracy of the determination coefficient R^2 is greater than 99.9, the structural bearing capacity of the measured GIs is considered in the calculation. The international KDF [34] is used to describe the influence of GIs on bearing capacity. Table 1 shows the relative deviation of the calculated results from the experiments and the corresponding GIs knockdown factor.

Table 1

Comparison between simulation and experiment

ID	Simulation (kN)	Experiment (kN)	Relative deviation (%)	KDF (%)	Buckling position
1	2737.3	2843.7	-3.74	88.04	$4\pi/3$
2	2898.7	2888.8	0.34	93.23	$2\pi/3$ and $4\pi/3$
3	2885.8	2817.4	2.43	92.81	0 and $2\pi/3$

The comparison shows two phenomena. One is that there is small deviation between the simulation and the experiment when the imperfection is taken into consideration. It indicates that considering the GIst method in this work can provide more accurate result. The other is that the positions of failure in all structures are different. Since the imperfection filed shows certain stochastic characterization, it introduces uncertainty in terms of the failure position and the magnitude of the critical load. It is worth to note that the failure happened in the weld line for all structures although the positions were not the same. The reason is that there is larger variation in term of the off-surface deviation.

Table 2

Statistics of peak off-surface deviation of single plate

	Convex amplitude	Concave amplitude
Sample data(mm)	0.33	-0.70
	0.33	-0.69
	0.42	-0.70
	0.23	-0.53
	0.32	-0.55
	0.35	-0.54
	0.45	-0.56
	0.35	-0.60
	0.25	-0.53
Mean value	0.338	-0.600
Standard deviation	0.071	0.077
Sensitivity $\overline{EE}$ (KN)	1530.97	1592.54

The maximum values of the outer protrusion and inner concave of each plate in the existing samples were counted.Based on the information of 9 plate samples, the general situation is estimated, and the peak deviation distribution of single plate is established.And the bearing capacity sensitivity of the two types of amplitudes is analyzed. Table 2 shows the analysis results and the statistical results of the peak off-surface deviation of the sample single plate.Under the condition of small sample, the Lilliefors test is applied, and when the significance level is greater than 0.05, the peak value distribution follows the normal distribution.The concave amplitude, that is, the minimum off-surface deviation, is more sensitive to load.It is used as the amplitude simplification standard for this group of samples.

4.2. Feature analysis and simplification of Fourier coefficients

There are thousands coefficients above which takes much simulation cost. The Fourier series is simplified reasonably according to the imperfection features to improve the efficiency. As discussed before, each amplitude of Fourier coefficients reflects the influence level of the order in the imperfection field. Fig.7 shows the amplitude of Fourier coefficients of each sample.

It is obvious that the value of γ_{kl} is relatively larger for smaller wave number and order than the larger wave number and order in Fig.7. It indicates that these parts dominantly contribute to the random field of imperfection.

Circumferential shapes under typical periods (l=2, 3, 6 and 9) are illustrated as Fig. 8 by ignoring the axial imperfection. The order of a wave represents the circular frequency of the wave. Fig. 8(a) shows the roundness deviation of the overall cylindrical structure; Fig. 8(b) shows the imperfection features with a single plate as a symmetric period, such as the imperfection at the weld. The other waveform reflect the periodic features of symmetry within a single plate, and the symmetric period is an integral multiple of the plate.

As shown in Fig.7, the periodic properties of axial waveform have no obvious rules. The coefficients with less axial wave number and relatively clear features account for a larger amplitude. Since the 0-order waveform reflects the radial deviation of the structure and has little effect on the axial bearing capacity, it is not discussed here. The corresponding imperfection features with larger coefficients are shown in Fig. 9. It is notable that the axial imperfection is obvious if the axial waveform is half wave or multiple entire waves. The superposition of half wave and multiple entire waves have less contribution to the structural imperfections.

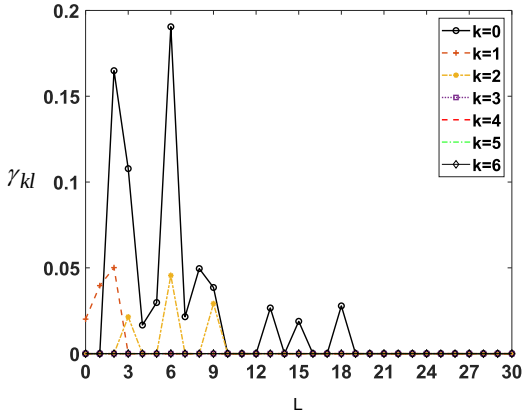

(a) Structure 1

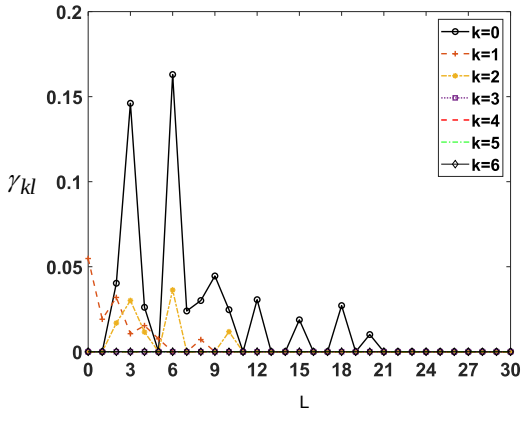

(b) Structure 2

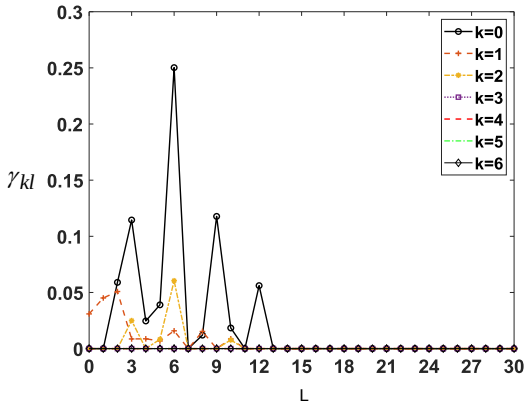

(c) Structure 3

Fig. 7 Fourier series amplitude of the sample shells

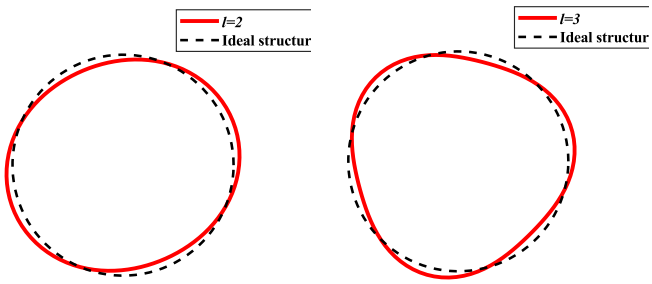

(a) $l=2$ (b) $l=3$

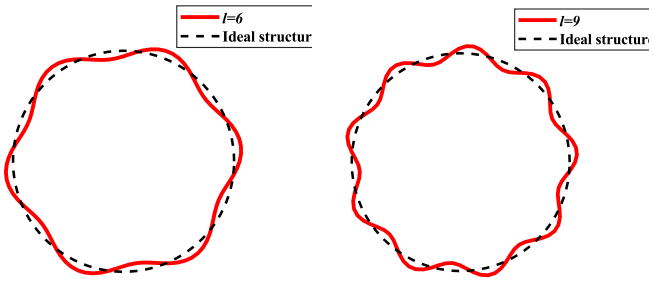

(c) $l=6$ (d) $l=9$

Fig. 8 Imperfection features of circumferential significant waveform

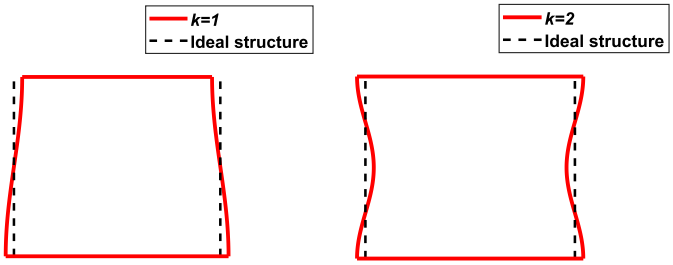

(a) $k=1$ (b) $k=2$

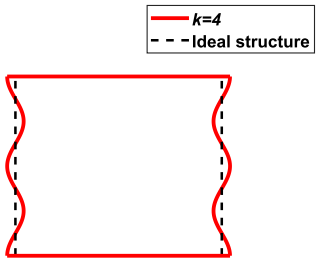

(c) $k=4$

Fig. 9 Imperfection features of axial significant waveform

The above features respectively construct the circumferential and axial imperfection bodies of welded plate structures, and reflect the overall law of imperfection features of such structures. The amplitude corresponding to each waveform reflects the difference of each product.The dominant Fourier coefficients are employed to reconstruct the structure. The reduction of the axial critical load of the structure under different waves is summarized. The results are shown in Table 3.

Table 3
The critical load characterized by single order coefficient

Order	Bearing load (kN)			Contribution of bearing capacity reduction(%)
	Shell 1	Shell 2	Shell 3	
$k=1$	3088.87	3100.47	3095.80	5.20
$k=2$	2823.00	2969.61	2971.57	68.29
$k=4$	3170.42	3156.34	3116.15	-13.99
$l=2$	3102.74	3089.46	3100.17	5.05
$l=3$	3100.63	3102.56	3098.49	3.42
$l=6$	2957.28	3029.39	2996.84	43.02
$l=9$	3155.28	3144.29	3140.09	-14.30

The results revealed that the off-surface deviation amplitude and period of the imperfection field are larger at lower order, which leads to larger reduction of the bearing load. As the order increases, it provides a smaller amplitude and period of the imperfection field. Among them, the two-order waveform of k=2 and l=6 contribute significantly to structural load reduction.The waveform signature of the structure during buckling are shown in Fig.10, which is manifested as 6 circumferential waves and 2 axial waves, consistent with the two-order waveform of k=2 and l=6. These two order imperfection signature are close to the buckling form of the structure, and can easily induce the structure to buckle under axial load.

The Fourier coefficients required to construct 1-m-diameter shell imperfections are more than 1000 terms.under $R^2 \geq 99.9\%$. The efficiencies about three simplification methods were analyzed and shown in Fig.11.

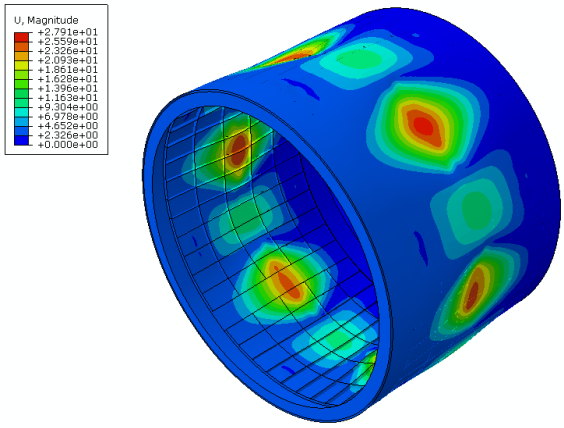

Fig. 10 Structural buckling waveform features

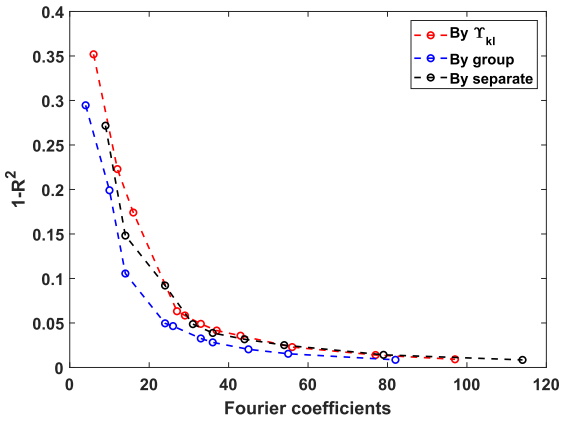

Fig. 11 Comparison of simplification efficiency

The number of Fourier coefficients required by the group set simplification method is lower than other two methods. Because the coefficients of each order A_{kl} and B_{kl} are different, some global small quantities will be retained in the simplified processing, resulting in low efficiency. Although γ_{kl} represents the amplitude of the two types of coefficients, the two types of coefficients of the same order are retained in the simplification process, so that part of the global small quantity is retained and the efficiency is reduced.However, set simplification method is more efficient because it selects from a global perspective and does not introduce global small quantity.

The coefficients of Fourier series are simplified considering the accuracy of the determination coefficient greater than 96%. The retained coefficients constitute the simplified GIs, and the comparison before and after is shown in Fig.12. The simplified imperfections ignore the items which influence the bearing capacity and keep the dominant items which can reduce the bearing capacity apparently.

In order to further test the rationality of simplification, the bearing capacity and buckling deformation of the structure were obtained which are tabulated in Table.4. The calculation deviation of structural bearing capacity compared with the full case is less than 1%, which meets the accuracy requirements. Moreover, the buckling mode and buckling position of the structure are highly coincident with the simulation results of real imperfections.

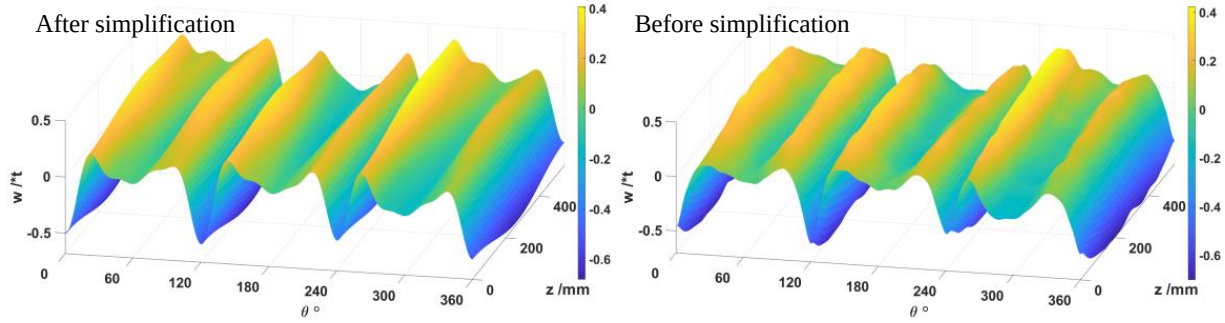

(a) Sample 1

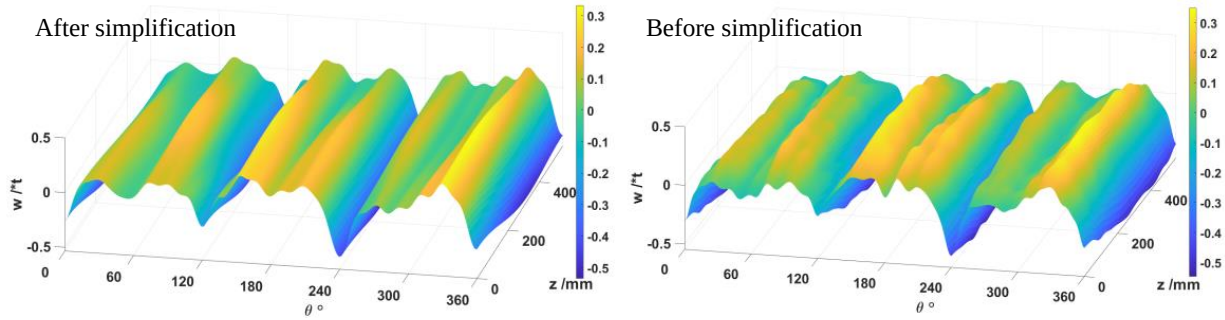

(b) Sample 2

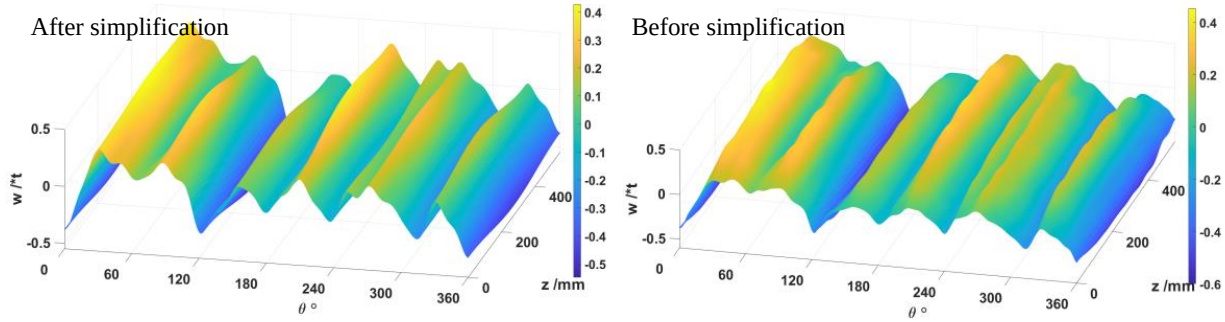

(c) Sample 3

Fig. 12 Comparison of simplification efficiency

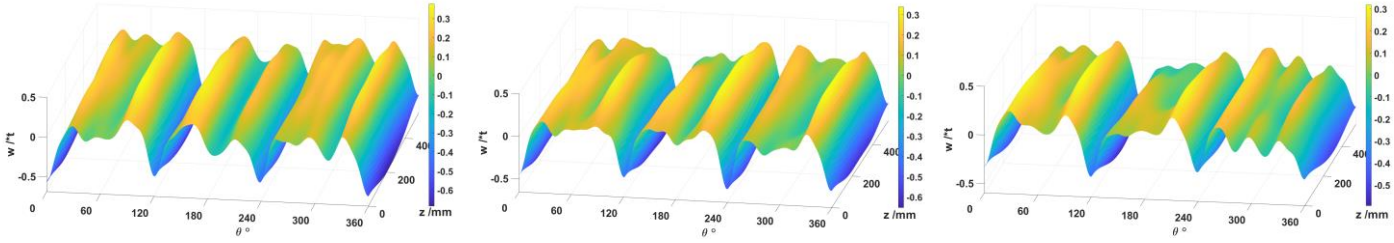

(a) (b) (c)

Fig. 13 Random field imperfection feature

Table 4
The bearing capacity of the structure after imperfection simplification

ID	Total Fourier coefficients	Coefficient of determination R^2	Bearing capacity(kN)	RP(%)	Buckling position
1	30	0.964	2783.1	0.3	$4\pi/3$
2	33	0.967	2874.8	0.8	$2\pi/3$ and $4\pi/3$
3	24	0.966	2906.8	0.7	0 and $2\pi/3$

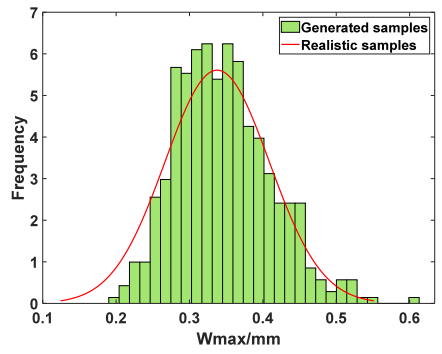

（a）Maximum statistics

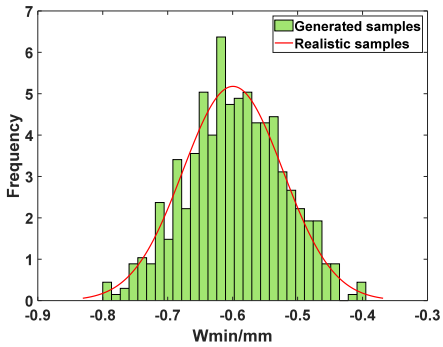

（b）Minimum statistics

Fig. 14 Distribution on the maximum off-surface deviation of random field

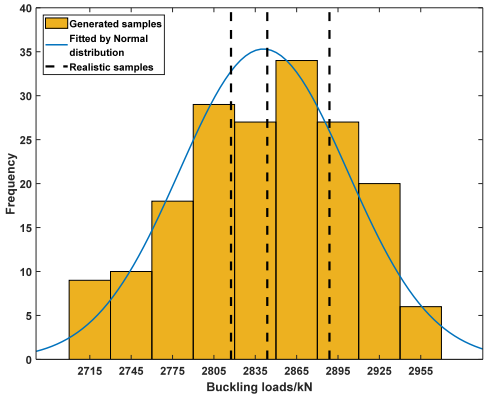

Fig. 15 Distribution on the bearing load

4.3. Imperfection random field-based bearing load prediction

Uniform sampling for imperfection field was carried out to reconstruct the structure for buckling analysis. The minimum off-surface deviation constraint is introduced in the imperfection feature field during sampling. 200 groups of imperfection characteristic fields were generated within 2 hours and the structures were reconstructed according to the sampling results.

According to the discussion above, the influence of imperfections on the bearing capacity is related to the features of imperfections and the amplitude of off-surface deviation. Three cases in the sample set were contoured to investigate the feature of the random field as shown in Fig.13. It presents the typical “M” shape for each part of the shell which is highly consistent with the actual samples.

The distribution about the maximum off-surface deviation of all random samples were shown in Fig.14. The results show that the minimum value is basically consistent with the sample distribution form, and the maximum value is slightly deviated from the decreasing direction of the deviation value under the sample distribution form. The majority of the results falls within the envelope of the sample probability density curve. The statistics of the maximum off-surface deviation of the test set are close to the sample state.

As shown in Fig.15, the results from the experiments all fall within the distribution range of the loading capacity of random fields.And it coincides with the high probability distribution. Using the Anderson-Darling test, when the significance level is greater than 0.05, the results are considered to follow normally distribution. According to the physical test results on the bearing capacity of the real sample, the mean and variance of the bearing capacity of the structure are predicted. Structural design orientated, the envelope of the structural load is realised by considering the confidence level of meeting the requirements based on the prediction of the load uncertainty. Under the normal distribution hypothesis of small sample, the mean and variance of the population are unknown. The confidence interval estimation on the mean and standard deviation can be expressed as:

$$\begin{aligned}\hat{\mu}&:\left(\overline{X}\pm\frac{S}{\sqrt{n}}t_{\alpha/2}(n-1)\right)\\ \hat{\sigma}&:\left(\frac{S\sqrt{n-1}}{\sqrt{\chi^2_{\alpha/2}(n-1)}},\frac{S\sqrt{n-1}}{\sqrt{\chi^2_{1-\alpha/2}(n-1)}}\right)\end{aligned}\tag{9}$$

Where $\overline{X}$ and S are the mean and standard deviation of the sample respectively. With the significance level $\alpha=1$, the confidence intervals for estimating the population mean and standard deviation are $\hat{\mu}\in[2760.32,2939.62]$ and $\hat{\sigma}\in[13.29,159.78]$, respectively. Under the imperfection random field, the mean μ=2839.3 and standard deviation σ=60.6 fall within the above confidence interval. The results clarify that the imperfection random field model proposed in this work can accurately reflect the influence of the surface detail on the bearing capacity.

5. Conclusion

In this paper, for the problem of uncertainty in the shape of welded thin-walled cylindrical shell structure of the panel, we innovatively put forward a small sub-sample-based Fourier series geometric imperfection random field construction method, and combined with the results of the strength test to carry out the load-bearing capacity of the target verification. Based on the typical surface imperfection characteristics of thin-walled cylindrical shells welded by panels in relation to the process, the sample expansion is realised using a single panel as a sample. From a completely new perspective, a dual defect imperfection uncertainty random field construction method based on the waveform and amplitude of the sample imperfection distribution is used, which ensures the adequacy of the sampling process and imposes constraints on the deviation of the results from the sample. The sampling test results match the experiments, verifying the accuracy of the method, and the following conclusions are drawn:

(1)The characterization of GIs by Fourier series in the traditional method requires a large number of coefficients, which is not conducive to random field modeling. The coefficient set reduction method proposed in this paper is applied, and the contribution degree of each order coefficient to the whole imperfection is taken as the reduction criterion. Under the premise of ensuring 99% accuracy of bearing capacity and consistent failure mode, more than 1,000 coefficients can be reduced to about 30, which greatly improves the characterization efficiency.

(2)According to the test results of the geometrical imperfections of welded cylindrical shell structures and the imperfection field data published in literature, the imperfection rules of each panel are consistent. By taking the smallest independent unit of the structure, the single wall panel, as the statistical sample of imperfection amplitude, a imperfection random field model is established to achieve sample expansion to a certain extent.

(3)Geometric imperfection feature sampling is carried out with Fourier series statistics of product samples, and imperfection magnitude constraints are carried out with statistics of panel samples to establish a geometric imperfection random field construction method. Tested by 200 sets of sampling data, the structural bearing capacity distribution under the random field model reasonably envelops the physical test results.

With the increase of the number of samples, the method has a tendency to grow in construction accuracy. The proposed method is a technical prerequisite for the simulation of thin-walled cylindrical shells' load-carrying capacity targeting in consideration of geometric imperfection random fields, and provides technical support for the realisation of scientific determination of the lower limit of structural strength and deviation based on the probabilistic method.

Acknowledgments

This work was supported by the National Natural Science Foundation of

China (Grant Nos. U2141217), and the Chinese pre-research project on Civil Aerospace Technologies (Grant Nos.305060504) .

References

[1] Chan S.L. and Chui P.T., Non-Linear Static and Cyclic Analysis of Steel Frames with Semi-Rigid Connections, Elsevier, New York, 2000.
[2] Liu S.W., Chan T.M., Chan S.L. and So. D.K.L., "Direct analysis of high-strength concrete-filled-tubular columns with circular & octagonal sections", Journal of Constructional Steel Research, 129, 301-314, 2017.
[1] Shi, Y.H., Fu, H.F., Xv, W.X. and Yang, F., "Research status and prospects on the strength variation coefficient of large diameter thin-walled structures" , Structure and Environment Engineering, 51, 1-12, 2024. (in Chinese)
[2] Jiao, P., Chen, Z., Tang, X., Su, W., and Wu, J., "Design of axially loaded isotropic cylindrical shells using multiple perturbation load approach–Simulation and validation", Thin-Walled Structures, 133, 1-16, 2018.
[3] Naraykin, O., Sorokin, F., and Kozubnyak, S., "Numerical Determination of the Splitting of Natural Frequencies of a Thin-Walled Shell with Small Nonaxisymmetric Imperfections of the Middle Surface", Mathematical Models and Computer Simulations, 15(5), 850-862, 2023.
[4] Teter, A., and Kolakowski, Z., "Interactive buckling of wide plates made of Functionally Graded Materials with rectangular stiffeners", Thin-Walled Structures, 171, 108750, 2022.
[5] Weingarten, V. I., Seide, P., and Peterson, J. P., "Buckling of thin-walled circular cylinders", No. NASA-SP-8007, 1968.
[6] Hilburger, M. W., Nemeth, M. P., and Starnes Jr, J. H., "Shell buckling design criteria based on manufacturing imperfection signatures", AIAA journal, 44(3), 654-663, 1968.
[7] Wang, B., Zhu, S., Hao, P., Bi, X., Du, K., Chen, B., Ma, X.,and Chao, Y. J., "Buckling of quasi-perfect cylindrical shell under axial compression: a combined experimental and numerical investigation", International Journal of Solids and Structures, 130, 232-247, 1968.
[8] Hühne, C., Rolfes, R., Breitbach, E., and Teßmer, J., "Robust design of composite cylindrical shells under axial compression—simulation and validation", Thin-walled structures, 46(7-9), 947-962, 2008.
[9] Wang, B., Hao, P., Li, G., Fang, Y., Wang, X., and Zhang, X., "Determination of realistic worst imperfection for cylindrical shells using surrogate model", Structural and Multidisciplinary Optimization, 48, 777-794, 2013.
[10] Schmidt, H., "Stability of steel shell structures: General Report", Journal of Constructional Steel Research, 55(1-3), 159-181, 2000.
[11] Arbocz, J., and Williams, J. G., "Imperfection surveys on a 10-ft-diameter shell structure", AIAA Journal, 15(7), 949-956, 1977.
[12] Elishakoff, I., and Arbocz, J. [1982] "Reliability of axially compressed cylindrical shells with random axisymmetric imperfections", International Journal of Solids and Structures, 18(7), 563-585.
[13] Wagner, H. N. R., Hühne, C., and Elishakoff, I., "Probabilistic and deterministic lower-bound design benchmarks for cylindrical shells under axial compression", Thin-Walled Structures, 146, 106451, 2020.
[14] Kepple, J., Herath, M. T., Pearce, G., Prusty, B. G., Thomson, R., and Degenhardt, R., "Stochastic analysis of imperfection sensitive unstiffened composite cylinders using realistic imperfection models", Composite Structures, 126, 159-173, 2015.
[15] Zhang, D., Chen, Z., Li, Y., Jiao, P., Ma, H., Ge, P., and Gu, Y., "Lower-bound axial buckling load prediction for isotropic cylindrical shells using probabilistic random perturbation load approach", Thin-Walled Structures, 155, 106925, 2020.
[16] Arbocz, J., and Hol, J. M. A. M., "Collapse of axially compressed cylindrical shells with random imperfections", AIAA journal, 29(12), 2247-2256, 1991.
[17] Gray, A., Wimbush, A., de Angelis, M., Hristov, P. O., Calleja, D., Miralles-Dolz, E., and Rocchetta, R., "From inference to design: A comprehensive framework for uncertainty quantification in engineering with limited information", Mechanical Systems and Signal Processing, 165, 108210, 2022.
[18] Hotelling, H. "Analysis of a complex of statistical variables into principal components", Journal of educational psychology, 24(6), 417, 1933.
[19] Ghanem, R. G., and Spanos, P. D., "Spectral stochastic finite-element formulation for reliability analysis", Journal of Engineering Mechanics, 117(10), 2351-2372, 1991.
[20] Li, C. C., and Der Kiureghian, A., "Optimal discretization of random fields", Journal of engineering mechanics, 119(6), 1136-1154, 1993.
[21] Lauterbach, S., Fina, M., and Wagner, W., "Influence of stochastic geometric imperfections on the load-carrying behaviour of thin-walled structures using constrained random fields", Computational Mechanics, 62, 1107-1125, 2018.
[22] Luo, Y., Zhan, J., Xing, J., and Kang, Z., "Non-probabilistic uncertainty quantification and response analysis of structures with a bounded field model", Computer Methods in Applied Mechanics and Engineering, 347, 663-678, 2019.
[23] Li, Z., Pasternak, H., and Geißler, K., "Buckling Analysis of Cylindrical Shells using Stochastic Finite Element Method with Random Geometric Imperfections", ce/papers, 5(4), 653-658, 2022.
[24] Yang, H., Feng, S., Hao, P., Ma, X., Wang, B., Xu, W., and Gao, Q., "Uncertainty quantification for initial geometric imperfections of cylindrical shells: A novel bi-stage random field parameter estimation method", Aerospace Science and Technology, 124, 107554, 2022.
[25] Fina, M., Weber, P., and Wagner, W., "Polymorphic uncertainty modeling for the simulation of geometric imperfections in probabilistic design of cylindrical shells", Structural Safety, 82, 101894, 2020.
[26] Schenk, C. A., and Schuëller, G. I., "Buckling analysis of cylindrical shells with random geometric imperfections", International journal of non-linear mechanics, 38(7), 1119-1132, 2003.
[27] Jianyu, L., Kun, Y., Bo, W., and Lili, Z., "A maximum entropy approach for uncertainty quantification of initial geometric imperfections of thin-walled cylindrical shells with limited data", Chinese Journal of Theoretical and Applied Mechanics, 55(4), 1028-1038, 2023.
[28] Wu, J., Luo, Y. F., and Wang, L., "Inversion algorithm for the geometric imperfection distribution of existing reticulated structures", Journal of Zhejiang University, 52(5), 864-872, 2018.
[29] Arbocz, J., and Hilburger, M. W., "Toward a probabilistic preliminary design criterion for buckling critical composite shells", AIAA journal, 43(8), 1823-1827, 2005.
[30] Hilburger, M. W. [2018] "On the development of shell buckling knockdown factors for stiffened metallic launch vehicle cylinders," In 2018 AIAA/ASCE/AHS/ASC structures, structural dynamics, and materials conference , pp. 1990.
[31] Lovejoy, A. E., Hilburger, M. W., and Gardner, N. W., "Test and analysis of full-scale 27.5-foot-diameter stiffened metallic launch vehicle cylinders", In 2018 AIAA/ASCE/AHS/ASC Structures, Structural Dynamics, and Materials Conference, 2018.
[32] Hilburger, M., Haynie, W., Lovejoy, A., Roberts, M., Norris, J., Waters, W., and Herring, H., "Sub-scale and full-scale testing of buckling-critical launch vehicle shell structures," In 53rd AIAA/ASME/ASCE/AHS/ASC Structures, Structural Dynamics and Materials Conference 20th AIAA/ASME/AHS Adaptive Structures Conference 14th AIAA, 2012.
[33] Hilburger, M., Lovejoy, A., Thornburgh, R., and Rankin, C., "Design and analysis of subscale and full-scale buckling-critical cylinders for launch vehicle technology development", In 53rd AIAA/ASME/ASCE/AHS/ASC Structures, Structural Dynamics and Materials Conference 20th AIAA/ASME/AHS Adaptive Structures Conference 14th AIAA , 2012.
[34] Hilburger, M. W., "Buckling of thin-walled circular cylinders", No. NASA/SP-8007-2020/REV 2, 2020.